

# Collision-Free Continuum Deformation Coordination of a Multi-Quadcopter System Using Cooperative Localization

Hamid Emadi<sup>1</sup>, Harshvardhan Uppaluru<sup>1</sup>, Hashem Ashrafiun<sup>2</sup>, and Hossein Rastgoftar<sup>1</sup>

**Abstract**—This paper integrates cooperative localization with continuum deformation coordination of a multi-quadcopter system (MQS) to assure safety and optimality of the quadcopter team coordination in the presence of position uncertainty. We first consider the MQS as a finite number of particles of a deformable triangle in a 3-D motion space and define their continuum deformation coordination as a leader-follower problem in which leader quadcopters can estimate (know) their positions but follower quadcopters rely on relative position measurements to localize themselves and estimate the leaders' positions. We then propose a navigation strategy for the MQS to plan and acquire the desired continuum deformation coordination, in the presence of measurement noise, disturbance, and position uncertainties, such that collision is avoided and rotor angular speeds of all quadcopters remain bounded. We show the efficacy of the proposed strategy by simulating the continuum deformation coordination of an MQS with eight quadcopters.

## I. INTRODUCTION

Unmanned vehicles have been widely used in military [1] and non-military applications such as data acquisition from hazardous environments [2] or agricultural farm fields [3], traffic surveillance applications [4], urban search and rescue [5], wildlife monitoring and exploration [6] and delivery tasks [7]. Global position estimation is a challenging problem for unmanned vehicles navigating in uncertain environments. Researchers have proposed feature-based [8] and landmark-based [9] simultaneous localization and mapping (SLAM) algorithms for mobile robot localization in unknown environments. For multi-agent localization, cooperative localization (CL) has been proposed to enable mobile agents to estimate their global positions by sharing odometry and relative position information. CL has been used in a wide variety of applications such as navigation of double-integrator multi-agents systems [10] and ground and aerial vehicles [11], search and rescue missions [12], and target tracking problems [13].

In CL, each agent is equipped with sensors, processing and communication capabilities which enables it to take relative measurements with respect to in-neighbor agents and distribute information to the fusion Center (FC) or only to the in-neighbor agents. These information are mostly noisy signals due to the measurement noises and dynamics of the system. CL uses different estimation approaches, such

as extended Kalman filters (EKF) [14], maximum likelihood [15], maximum a posteriori (MAP) [16], to estimate global positions of member agents of a team by filtering the relative position measurements provided in a distributed fashion.

In this work, we combine CL and continuum deformation coordination approach [17], [18] to safely plan the group coordination of a multi-quadcopter system (MQS) in the presence of position uncertainty. We consider a group of MQS moving in a 3-D motion space with the desired coordination defined by a non-singular deformation mapping called *homogeneous transformation*. Homogeneous deformation coordination is defined as a leader-follower problem; an  $n$ -D continuum deformation of a quadcopters are guided by  $n + 1$  leader agents, located at vertices of a  $n$ -D simplex for all time  $t$  ( $n \in \{1, 2, 3\}$  denotes the dimension of the continuum deformation coordination). In this work, without loss of generality, quadcopters are considered as particles of a 2-D deformable body coordinating in an obstacle-laden motion space, thus,  $n = 2$ , and the desired continuum deformation coordination is defined by three leaders. While the existing homogeneous transformation coordination [17], [18] model quadcopters with deterministic dynamics, this paper studies continuum deformation coordination of the MQS in the presence of position uncertainty, measurement noise, and disturbance. In particular, we assume leaders can localize themselves with respect to the environment but followers localize themselves, estimate leaders position, and acquire their desired trajectories by cooperative localization. While the MQS continuum deformation coordination is planned such that travel distance and time are minimized in an obstacle-laden environment, we formally specify and verify safety of the MQS continuum deformation in the presence of global position uncertainty to assure angular speed of no quadcopter violates a certain upper limit, and collision is avoided.

The organization of the paper is as follows. Section II presents the problem formulation. Section III presents the collective dynamics of MQS. Section IV presents the state estimation approach and KF. Section V discusses the continuum deformation planning in the presence of position uncertainty. Section VI gives the simulation of the proposed method on a network of 8 quadcopters, and followed by Conclusion in Section VII.

## II. PROBLEM STATEMENT

We consider collective motion of an MQS in an obstacle-laden motion space where quadcopters are identified by

<sup>1</sup>H. Emadi, H. Uppaluru, and H. Rastgoftar are with the Aerospace and Mechanical Engineering Department at University of Arizona, AZ, USA, Emails: {hamidemadi, huppaluru, hrastgoftar}@arizona.edu

<sup>2</sup>H. Ashrafiun is with the Mechanical Engineering Department at Villanova University, PA, USA 19085, Email: hashem.ashrafiun@villanova.edu

unique index numbers identified by set  $\mathcal{V} = \{1, \dots, N\}$ . We treat the quadcopters as particles of a 2-D deformable triangle with three leaders defined by  $\mathcal{V}_L = \{1, 2, 3\}$  and  $N - 3$  followers defined by set  $\mathcal{V}_F = \mathcal{V} \setminus \mathcal{V}_L = \{4, \dots, N\}$ . Suppose that an MQS is represented by a directed graph  $G(\mathcal{V}, \mathcal{E})$  (see Fig 1a), where  $\mathcal{V}$  is the node set, and the edge set  $\mathcal{E} \subseteq \mathcal{V} \times \mathcal{V}$  is defined as a set of pairs  $(i, j)$  connecting node  $i$  to node  $j$  ( $i, j \in \mathcal{V}$ ). Specifically, edge  $(i, j)$  physically means that agent  $j$  can take the relative measurement of agent  $i$ . It should be noted that self loop in the network implies that the corresponding agent can receive GPS signals and can measure its global states. Without loss of generality, we assume that each follower has 3 in-neighbor agent in the network. We denote the in-neighbor agents of agent  $i$  as set  $\mathcal{N}_i = \{i_1, i_2, i_3\}$ .

Let  $\mathbf{r}_i(t) = [x_i(t) \ y_i(t) \ z_i(t)]^T$  and  $\mathbf{r}_{i,d}(t) = [x_{i,d}(t) \ y_{i,d}(t) \ z_{i,d}(t)]^T$  denote the global position and desired position vector of agent  $i \in \mathcal{V}$  at time  $t$ , respectively. Let  $\mathbf{r}_{i,0} = [x_{i,0} \ y_{i,0} \ 0]^T$  denote the reference position of agent  $i \in \mathcal{V}$  in  $x - y$  plane.

We assume that the desired trajectory of each quadcopter  $i \in \mathcal{V}_L$  is obtained from the following equation:

$$\mathbf{r}_{i,d}(t) = \mathbf{Q}(t, t_0) (\mathbf{r}_{i,0} - \mathbf{d}(t_0)) + \mathbf{d}(t) \quad t \in [t_0, t_f] \quad (1)$$

where  $\mathbf{Q}(t, t_0) \in \mathbb{R}^{3 \times 3}$  is the Jacobian matrix and  $\mathbf{d}(\cdot) \in \mathbb{R}^3$  is the rigid body displacement vector [18].

We assume that the leaders' desired trajectories are given (see section V), and we define the desired trajectory of the followers as a weighted summation of leaders' position. For every quadcopter  $i \in \mathcal{V}_F$ , we define three parameters  $\alpha_{i,1}$ ,  $\alpha_{i,2}$ , and  $\alpha_{i,3}$  ( $\sum_{j=1}^3 \alpha_{i,j} = 1$ ), based on reference position of quadcopter  $i$  and the leaders' reference positions as follows:

$$\begin{bmatrix} \alpha_{i,1} \\ \alpha_{i,2} \\ \alpha_{i,3} \end{bmatrix} = \begin{bmatrix} x_{1,0} & x_{2,0} & x_{3,0} \\ y_{1,0} & y_{2,0} & y_{3,0} \\ 1 & 1 & 1 \end{bmatrix}^{-1} \begin{bmatrix} x_{i,0} \\ y_{i,0} \\ 1 \end{bmatrix}, \quad \forall i \in \mathcal{V}_F. \quad (2)$$

The collective motion of the MQS is defined as a leader-follower problem in which the desired trajectory of quadcopter  $i \in \mathcal{V}_F$ , denoted by  $\mathbf{r}_{i,d}$ , are given by

$$\mathbf{r}_{i,d}(t) = \sum_{j \in \mathcal{V}_L} \alpha_{i,j} \mathbf{r}_{j,d}(t). \quad (3)$$

In Fig. 1a,  $\alpha_{i,j}$ 's are represented for a group of 8 quadcopters. Directed graph  $G(\mathcal{V}, \mathcal{E})$  is also shown in Fig. 1a. Fig. 1b shows the desired configuration of an MQS on 2-D simplex in 3-D space at time  $t$ .

The main objective of this work is to design distributed coordination control for an MQS to safe travel in an obstacle-laden environment (see Fig. 2). We suppose that the leaders have access to the GPS signals and followers can only measure the relative pose respect to in-neighbor agents. We consider two safety conditions. First, we assume that the rotor speeds of every quadcopter must not exceed  $\omega_r^{max}$ . This safety condition can be formally specified by

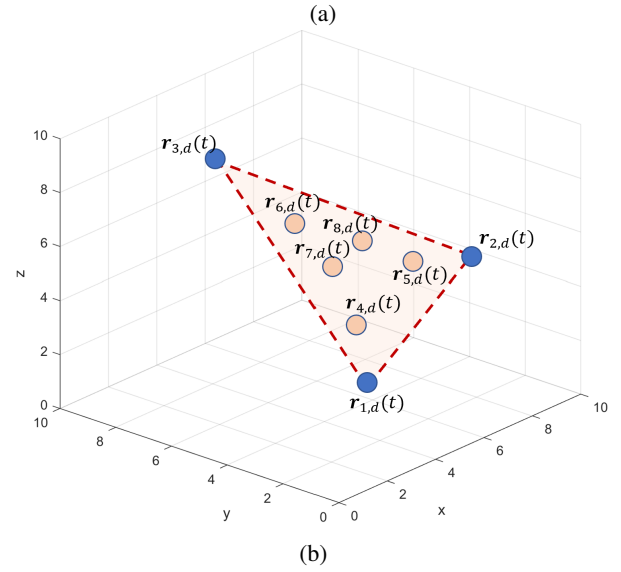
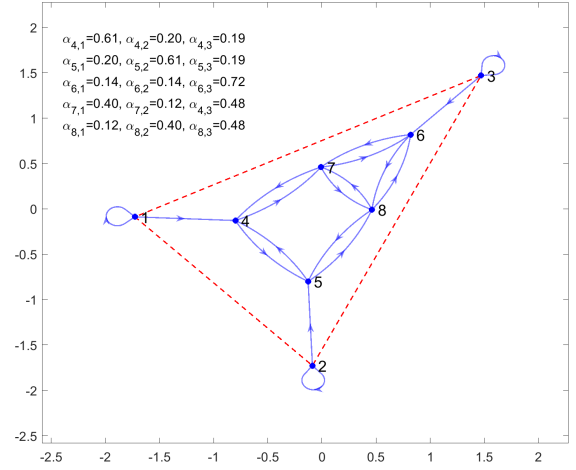


Fig. 1: (a) Blue arrows show the directed graph of MQS, and red dashed lines show the leaders' reference configuration in the  $x - y$  plane.  $\alpha_{i,j}$  are shown in the plot. (b) Agents' configuration on 2-D simplex in 3-D space at time  $t$

$$0 < \omega_{r,i,j}(t) \leq \omega_r^{max}, \quad \forall i \in \mathcal{V}, j \in \{1, \dots, 4\}, \forall t \geq t_0 \quad (4)$$

where  $\omega_{r,i,j}(t)$  is the angular speed of rotor  $j \in \{1, \dots, 4\}$  of quadcopter  $i \in \mathcal{V}$  at time  $t \geq t_0$ . Moreover, trajectory of each quadcopter should be close enough to the corresponding desired trajectory. In particular, following condition should be satisfied for all agents  $i \in \mathcal{V}$  at all  $t$ :

$$\|\mathbf{r}_i(t) - \mathbf{r}_{i,d}(t)\| < \delta \quad \forall i \in \mathcal{V}, \forall t \geq t_0 \quad (5)$$

where  $\delta$  is the distance threshold value between desired and actual trajectories.

### III. COLLECTIVE DYNAMICS OF MQS

In this section, we present the collective dynamics of an MQS in 3-D space. We consider the motion of MQS as

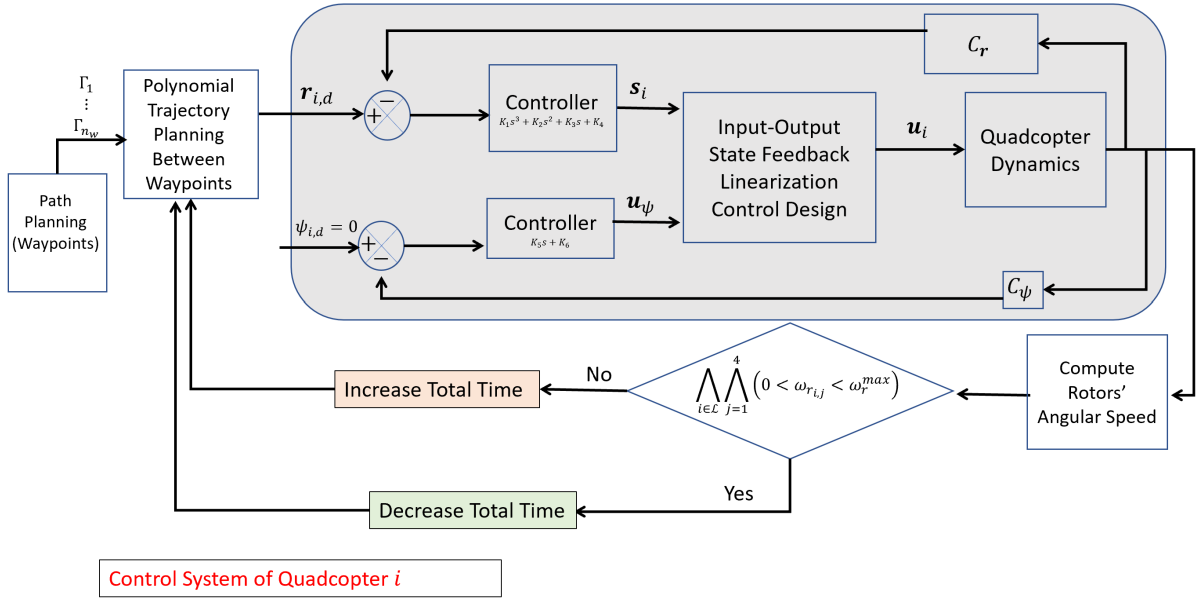


Fig. 2: Block diagram of MQS coordination control with the proposed method

particles of a 2-D continuum deformable body guided by 3 leaders. We assume that each agent  $i \in \mathcal{V}_L$  is equipped with proprioceptive sensors that can measure the global position. Moreover, we assume that each agent  $i \in \mathcal{V}_F$  can only measure the relative position with respect to the in-neighbor agents.

We assume that the leaders know the desired trajectories of (1), and we define the desired trajectory of the followers as a weighted summation of leaders' position in the following form:

$$\mathbf{r}_{i,d}(t) = \sum_{j=1}^3 \alpha_{i,j} \mathbf{r}_j(t), \quad t \in [t_0, t_f] \quad \forall i \in \mathcal{V}_F \quad (6)$$

where  $\alpha_{i,1}, \alpha_{i,2}$  and  $\alpha_{i,3}$  are positive numbers associated to agent  $i$ , and defined in (2).

Consequently, weight matrix  $\mathbf{W} \in \mathbb{R}^{N \times N}$ , defined based on the position of the quadcopters, can be written as

$$\mathbf{W} = \begin{cases} w_{i,j} & i \in \mathcal{V}_F, j \in \mathcal{V}_L \\ 0 & \text{otherwise} \end{cases} \quad (7)$$

From the above definition, matrix  $\mathbf{W}$  can be partitioned in the form of

$$\mathbf{W} = \begin{bmatrix} \mathbf{0}_{3 \times 3} & \mathbf{0}_{3 \times N-3} \\ \mathbf{W}_0 & \mathbf{0}_{N-3 \times N-3} \end{bmatrix} \quad (8)$$

where  $\mathbf{W}_0 \in \mathbb{R}^{N-3 \times 3}$  is defined as

$$\mathbf{W}_0 = \begin{bmatrix} \alpha_{4,1} & \alpha_{4,2} & \alpha_{4,3} \\ \vdots & \vdots & \vdots \\ \alpha_{N,1} & \alpha_{N,2} & \alpha_{N,3} \end{bmatrix} \quad (9)$$

We define matrix  $\mathbf{L}$  as

$$\mathbf{L} = \mathbf{W} - \mathbf{I}_N. \quad (10)$$

Let  $\mathbf{X} = \text{vec}([\mathbf{r}_1 \dots \mathbf{r}_N]^T)$  be the concatenation of position vector of all agents. The external dynamics of

all quadcopters (see equation (51)) can be written in the following form:

$$\frac{d}{dt} \begin{pmatrix} \mathbf{X} \\ \dot{\mathbf{X}} \\ \ddot{\mathbf{X}} \\ \dddot{\mathbf{X}} \end{pmatrix} = \mathbf{A}_{SYS} \begin{bmatrix} \mathbf{X} \\ \dot{\mathbf{X}} \\ \ddot{\mathbf{X}} \\ \dddot{\mathbf{X}} \end{bmatrix} + \mathbf{B}_{SYS} \begin{bmatrix} \mathbf{S}_L \\ \dot{\mathbf{S}}_L \\ \ddot{\mathbf{S}}_L \\ \dddot{\mathbf{S}}_L \end{bmatrix} \quad (11)$$

$$\mathbf{Y} = \mathbf{C}_{SYS} [\mathbf{X}^T \quad \dot{\mathbf{X}}^T \quad \ddot{\mathbf{X}}^T \quad \dddot{\mathbf{X}}^T]^T \quad (12)$$

where  $\mathbf{A}_{SYS} \in \mathbb{R}^{12N \times 12N}$ ,  $\mathbf{B}_{SYS} \in \mathbb{R}^{12N \times 12N}$  and  $\mathbf{C}_{SYS} \in \mathbb{R}^{36(N-2) \times 12N}$  are defined as

$$\mathbf{A}_{SYS} = \begin{bmatrix} \mathbf{0}_{3N \times 3N} & \mathbf{I}_{3N} & \mathbf{0}_{3N \times 3N} & \mathbf{0}_{3N \times 3N} \\ \mathbf{0}_{3N \times 3N} & \mathbf{0}_{3N \times 3N} & \mathbf{I}_{3N} & \mathbf{0}_{3N \times 3N} \\ \mathbf{0}_{3N \times 3N} & \mathbf{0}_{3N \times 3N} & \mathbf{0}_{3N \times 3N} & \mathbf{I}_{3N} \\ K_4 \mathbf{I}_3 \otimes \mathbf{L} & K_3 \mathbf{I}_3 \otimes \mathbf{L} & K_2 \mathbf{I}_3 \otimes \mathbf{L} & K_1 \mathbf{I}_3 \otimes \mathbf{L} \end{bmatrix} \quad (13)$$

$$\mathbf{B}_{SYS} = \begin{bmatrix} \mathbf{0}_{9N \times 9} & \mathbf{0}_{9N \times 9} & \mathbf{0}_{9N \times 9} & \mathbf{0}_{9N \times 9} \\ K_4 \mathbf{I}_3 \otimes \mathbf{L}_0 & K_3 \mathbf{I}_3 \otimes \mathbf{L}_0 & K_2 \mathbf{I}_3 \otimes \mathbf{L}_0 & K_1 \mathbf{I}_3 \otimes \mathbf{L}_0 \end{bmatrix} \quad (14)$$

$$\mathbf{C}_{SYS} = \mathbf{I}_{12} \otimes \mathbf{C}_0 \quad (15)$$

where  $\mathbf{L}_0 \in \mathbb{R}^{N \times 3}$  is

$$\mathbf{L}_0 = \begin{bmatrix} \mathbf{I}_3 \\ \mathbf{0}_{N-3 \times 3} \end{bmatrix} \quad (16)$$

$\mathbf{S}_L$  is defined as concatenation of desires trajectories of leaders as follows:

$$\mathbf{S}_L = \text{vec}([\mathbf{r}_{1,d} \quad \mathbf{r}_{2,d} \quad \mathbf{r}_{3,d}]^T) \quad (17)$$

$\mathbf{C}_0 \in \mathbb{R}^{3(N-2) \times N}$  is a matrix with the  $ij^{\text{th}}$  entry  $C_{0i,j}$  defined in the following way:

$$C_{0i,j} = \begin{cases} 1 & i = j, j \in \mathcal{V}_L \\ 1 & (j,i) \in \mathcal{E}, j \in \mathcal{V}_F \\ -1 & i = j, j \in \mathcal{V}_F \\ 0 & \text{otherwise} \end{cases} \quad (18)$$

We define  $\mathbf{Y}_d = \text{vec} \left( \begin{bmatrix} \mathbf{r}_{1,d} & \dots & \mathbf{r}_{N,d} \end{bmatrix}^T \right)$ . Vector  $\mathbf{Y}_d$  and  $\mathbf{S}_L$  are related as

$$\mathbf{Y}_d = (\mathbf{I}_3 \otimes \mathbf{H}) \mathbf{S}_L. \quad (19)$$

where  $\mathbf{H} = -\mathbf{L}^{-1} \mathbf{L}_0$  [17].

Now, by defining  $\mathbf{E}(t) = \mathbf{Y}(t) - \mathbf{Y}_d(t)$ , the error dynamics can be written in the form of

$$\frac{d}{dt} \begin{pmatrix} \mathbf{E} \\ \dot{\mathbf{E}} \\ \ddot{\mathbf{E}} \\ \dddot{\mathbf{E}} \end{pmatrix} = \mathbf{A}_{SYS} \begin{pmatrix} \mathbf{E} \\ \dot{\mathbf{E}} \\ \ddot{\mathbf{E}} \\ \dddot{\mathbf{E}} \end{pmatrix} + \begin{bmatrix} \mathbf{0} \\ \mathbf{0} \\ \mathbf{0} \\ \mathbf{I}_3 \otimes \mathbf{H}^T \end{bmatrix} \ddot{\mathbf{S}}_L \quad (20)$$

#### IV. STATE ESTIMATION OF MQS

In this section, we present the Kalman Filter state estimation algorithm following [19]. We consider a centralized scenario in which all agents share their measurements to a FC. Collective dynamics of the system is presented in (11). Note that leaders can measure their states, and followers can only measure the relative states of the in-neighbor agents. Matrix  $\mathbf{C}_0$  in (12) represents the explicit form of the absolute and the relative measurements in the network  $G$ .

In the first step, we discretize the continuous dynamics of (11). Suppose that sensors are sampling every  $\Delta t$  second. Discretizing the continuous state space model (11) and (12) lead to the following discrete approximation model

$$\begin{aligned} \mathbf{x}_{[k+1]} &= (\mathbf{A}_{SYS} \Delta t + \mathbf{I}) \mathbf{x}_{[k]} + (\mathbf{B}_{SYS} \Delta t) \mathbf{u}_{[k]} + \eta_{[k]} \mathbf{1} \\ \mathbf{y}_{[k+1]} &= \mathbf{C}_{SYS} \mathbf{x}_{[k]} + \nu_{[k]} \end{aligned} \quad (22)$$

where  $\mathbf{x}_{[k]}$ ,  $\mathbf{u}_{[k]}$  and  $\mathbf{y}_{[k]}$  represent the state vector, the control input vector and the measurement vector at time-step  $k$ , respectively, in in (11),(12).  $\eta_{[k]}$  and  $\nu_{[k]}$  are process noise and measurement noise, respectively. We assume that  $\eta_{[k]}$  and  $\nu_{[k]}$  are zero-mean independent white Gaussian processes with known covariances  $\mathbf{Q}_{[k]}$ ,  $\mathbf{R}_{[k]}$ , respectively. For each time step the Kalman filter is given by the following expressions:

$$\mathbf{P}_{[k+1]}^- = (\mathbf{A}_{SYS} \Delta t + \mathbf{I}) \mathbf{P}_{[k]}^+ (\mathbf{A} \Delta t + \mathbf{I})^T + \mathbf{Q}_{[k]} \quad (23)$$

$$\mathbf{K}_{[k+1]} = \mathbf{P}_{[k+1]}^- \mathbf{C}_{SYS}^T \left( \mathbf{C}_{SYS} \mathbf{P}_{[k+1]}^- \mathbf{C}_{SYS}^T + \mathbf{R}_{[k+1]} \right)^{-1} \quad (24)$$

$$\mathbf{x}_{[k+1]}^- = (\mathbf{A}_{SYS} \Delta t + \mathbf{I}) \mathbf{x}_{[k]}^+ + (\mathbf{B}_{SYS} \Delta t) \mathbf{u}_{[k]} \quad (25)$$

$$\mathbf{x}_{[k+1]}^+ = \mathbf{x}_{[k+1]}^- + \mathbf{K}_{[k+1]} (\mathbf{y}_{[k+1]} - \mathbf{C} \mathbf{x}_{[k+1]}^-) \quad (26)$$

$$\mathbf{P}_{[k+1]}^+ = (\mathbf{I} - \mathbf{K}_{[k+1]} \mathbf{C}_{SYS}) \mathbf{P}_{[k+1]}^- \quad (27)$$

where “+”, “-” refer to the prior and posterior estimation, respectively. That is to say, “+”, “-” correspond to the estimation after and before we process the measurement at time step  $k$ , respectively.  $\mathbf{P}_{[k]}$ ,  $\mathbf{K}_{[k]}$  represent the error estimation covariance and Kalman filter gain at time step  $k$ , respectively.

#### V. PATH PLANNING

We use the A\* search method [20] to path planning of the leaders in an obstacle-laden environment (see Fig.3). Deploying A\* search method results to a line-graph in which the node set represents the waypoints, and edge set represents the path segment between waypoints. We denote the position of waypoints by  $\Gamma_1, \dots, \Gamma_n$ . We assume that each quadcopter starts with zero velocity and zero acceleration at start point  $\Gamma_i$ , and reaches to the end point  $\Gamma_{i+1}$  of each segment with zero velocity and zero acceleration. We consider a trajectory of a quadcopter as a polynomial function of time with zero velocity and acceleration at  $\Gamma_i$  and  $\Gamma_{i+1}$ . This results to the desired trajectories of the leaders which satisfy (1) as follows:

$$\mathbf{r}_{i,d}^j(t) = (1 - \beta(t)) \Gamma_j + \beta(t) \Gamma_{j+1} \quad (28)$$

where  $\beta(t) = \frac{6}{T_j^5} t^5 - \frac{15}{T_j^4} t^4 + \frac{10}{T_j^3} t^3$ , and superscript  $j$  in  $\mathbf{r}_{i,d}^j(t)$  denotes the  $j^{\text{th}}$  path segment between  $\Gamma_j$  and  $\Gamma_{j+1}$ . We denote the total travelling time by  $T$ ; we linearly allocate travelling time  $T_j$  to the path segment between waypoints  $\Gamma_j$  and  $\Gamma_{j+1}$  based on the travelling distance between  $\Gamma_j$  and  $\Gamma_{j+1}$ . From (20), the tracking error can be written as

$$\begin{pmatrix} \mathbf{E} \\ \dot{\mathbf{E}} \\ \ddot{\mathbf{E}} \\ \dddot{\mathbf{E}} \end{pmatrix} = \int_{t_0}^t e^{\mathbf{A}_{SYS}(t-\eta)} \begin{bmatrix} \mathbf{0} \\ \mathbf{0} \\ \mathbf{0} \\ \mathbf{I}_3 \otimes \mathbf{H}^T \end{bmatrix} \ddot{\mathbf{S}}_L d\eta \quad (29)$$

From the above expression, as  $T_j$  tends to infinity,  $\mathbf{E}$  also tends to 0. This leads to the fact that there exists an optimal time  $T^*$  for give  $\delta$  such that safety condition (5) is satisfied for all time.

In order to find the optimal traveling time for MQS subjected to that safety conditions (4) and (5), we use bisection method. We initiate with a large  $T$  such that (4) and (5) are satisfied. Using the bisection method, we keep updating  $T$  until one of the safety conditions is violated. We denote the optimal time by  $T^*$ .

#### VI. SIMULATION

In this section, we consider an MQS containing 8 quadcopters labeled as  $\mathcal{V} = \{1, \dots, 8\}$ . In order to acquire the continuum deformation coordination, We consider 3 leaders in this group, labeled as  $\mathcal{V}_L = \{1, 2, 3\}$ , and the rest of agents are considered as followers  $\mathcal{V}_F = \{4, \dots, 8\}$ . A directed graph  $G(\mathcal{V}, \mathcal{E})$  is generated based on proximity for local relative measurements (see Fig. 1a). We assume that leaders are equipped by proprioceptive sensors which enable to acquire the global state vector measurements at each time step. On the other hand, each follower can only measure the relative states with respect to its neighbors (e.g. agent 4 can take the measurements relative to agents 1, 5 and 7). Note that self-loop in the network implies that the corresponding agent can measure its global states. Quadcopters' specification are listed in Table I.

We consider the standard deviation of 0.1 for process noise  $Q$  and measurement noise  $R$ . Sampling time in our simulation is 0.01 sec. Fig. 4 shows the trajectories of the MQS

$m$	$g$	$l$	$I_x$
0.468	9.81	0.225	$4.856 \times 10^{-3}$
$I_y$	$I_z$	$b$	$k$
$4.856 \times 10^{-3}$	$8.801 \times 10^{-3}$	$2.98 \times 10^{-6}$	$1.14 \times 10^{-7}$

TABLE I: Quadcopters' specification

from  $\Gamma_2$  to  $\Gamma_3$ . We choose  $K_1 = 10, K_2 = 35, K_3 = 50$  and  $K_4 = 35$ . Blue dashed lines show the actual trajectories of the agents, and solid green lines show the desired trajectories of 3 leaders. As shown in Fig. 4, followers are contained in the triangle, formed by the three leaders. Fig. 1 shows the estimation and tracking error of agent 4 (a follower agent).

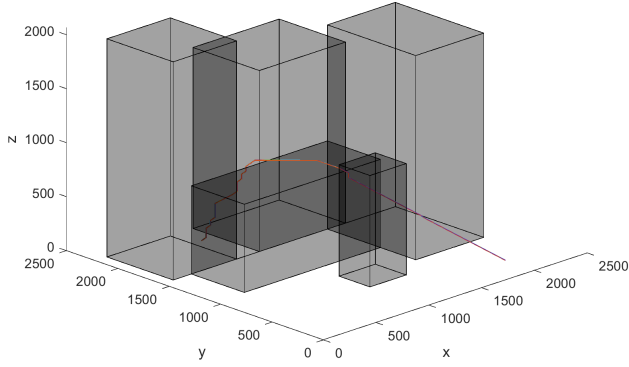


Fig. 3: An obstacle-laden environment. Leaders' desired paths which is generated from the approach discussed in Section V, also shown in the plot

We choose  $\delta = 0.5$  in the safety condition (5), and  $\omega_{r_{\max}} = 750$  in safety condition (4). Using the bisection method,  $T^*$  is computed as 640 seconds. Fig. 6 shows the angular speed of rotor 1 for quadcopter 4. As shown in Fig. 6,  $\omega_r$  is not exceeding the  $\omega_{r_{\max}} = 750$ . Fig. 7 and 8 show the roll, pitch and yaw angle of quadcopter 4 and  $x, y$  and  $z$  components of quadcopters for  $t \in [0, T^*]$ , respectively.

## VII. CONCLUSION

We developed a framework for continuum deformation coordination of MQS through simultaneous cooperative localization. We provided the collective dynamics of the quadcopters in which the input is the leader's desired trajectory, and the output only contains the estimated global states of the leaders and the estimated relative states of the followers respect to in-neighbor agents. We used Kalman Filter for state estimation of the collective motion system. In this work, we used FC to collect and distribute the information to the network. As a part of the future work we plan to develop a decentralized method for state estimation and coordination of quadcopters.

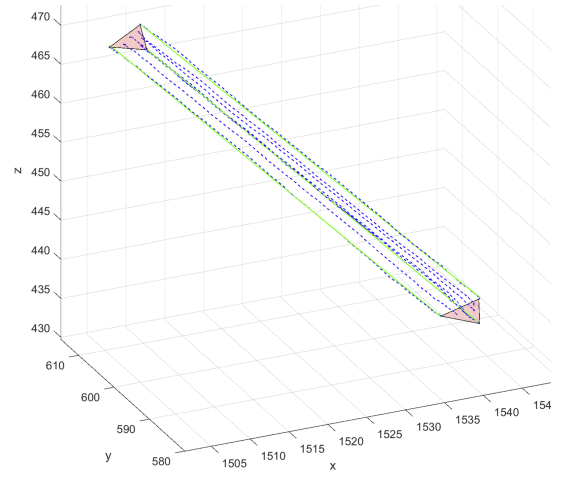


Fig. 4: Actual (green lines) and desired (blue lines) trajectories of MQS for the path segment between waypoints  $\Gamma_2, \Gamma_3$ .

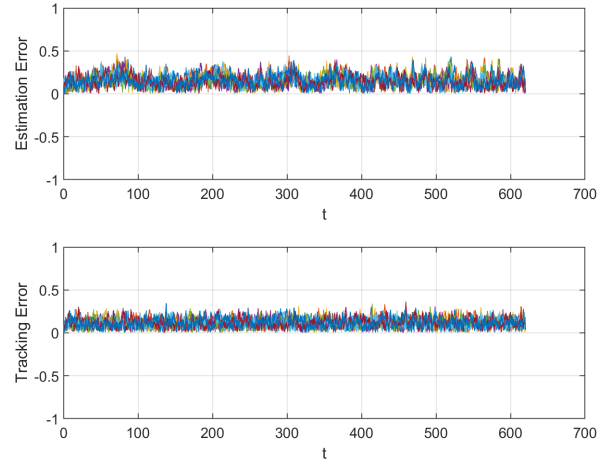


Fig. 5: Tracking error and estimation error for all agents

## VIII. ACKNOWLEDGEMENT

This work has been supported by the National Science Foundation under Award Nos. 2133690 and 1914581.

## APPENDIX

### A. Mathematical Modeling of Quadcopters and Trajectory Tracking Control

In this work, we consider the following assumptions in mathematical modeling of quadcopter motions.

*Assumption 1:* Quadcopter is a symmetrical rigid body with respect to the axes of body-fixed frame.

*Assumption 2:* Aerodynamic loads are neglected due to low speed assumption for quadcopters.

Let  $\hat{i}, \hat{j}, \hat{k}$  be the base vectors of inertial coordinate system, and  $\hat{i}_b, \hat{j}_b, \hat{k}_b$  be the base unit vectors of a body-fixed coordinate system whose origin is at the center of mass of the quadcopter. In this section, for convenience, we omitted  $i$  subscript of  $i^{\text{th}}$  quadcopter in the governing equations. The attitude of the quadcopter is defined by three

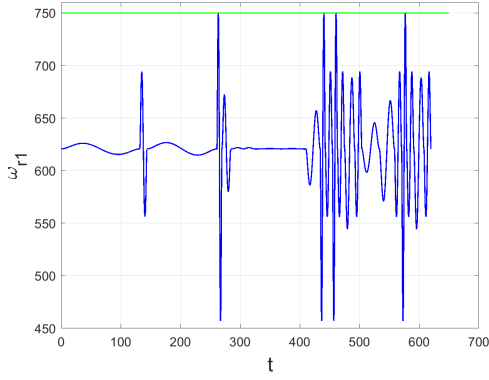


Fig. 6: Blue line shows the angular speed  $\omega_{r1}$  during the total travelling time. Green line shows the upper limit  $\omega_{r1}^{\max}$ .

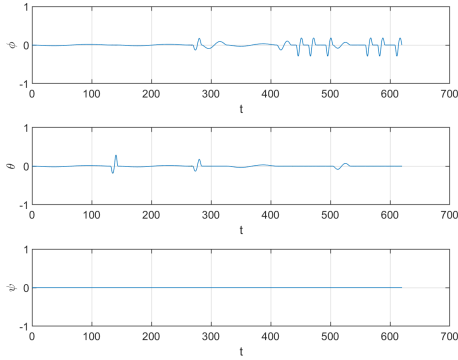


Fig. 7:  $\phi, \theta$  and  $\psi$  for agent 4.

Euler angles  $\phi, \theta$  and  $\psi$  as roll angle, pitch angle and yaw angle, respectively. In this work, we use 3-2-1 standard Euler angles to determine orientation of the quadcopter. Therefore, the rotation matrix between fixed-body frame and the inertial frame can be written as

$$\mathbf{R}(\phi, \theta, \psi) = \mathbf{R}(\phi, 0, 0)\mathbf{R}(0, \theta, 0)\mathbf{R}(0, 0, \psi) \quad (30)$$

$$= \begin{bmatrix} c_\phi c_\psi & s_\theta c_\psi s_\phi - s_\psi c_\phi & s_\theta c_\psi c_\phi + s_\psi s_\phi \\ c_\phi s_\psi & s_\theta s_\psi s_\phi + c_\psi c_\phi & s_\theta s_\psi c_\phi - c_\psi s_\phi \\ -s_\theta & c_\theta s_\phi & c_\theta c_\phi \end{bmatrix} \quad (31)$$

where  $s(\cdot) = \sin(\cdot), c(\cdot) = \cos(\cdot)$ . Let  $\mathbf{r} = [x \ y \ z]^T$  denote the position of the center of mass of the quadcopter in inertial frame, and  $\boldsymbol{\omega} = [\omega_x \ \omega_y \ \omega_z]^T$  denote the angular velocity of the quadcopter represented in the fixed-body frame.

Using the Newton-Euler formulas, equations of motion of a quadcopter can be written in the following form:

$$\ddot{\mathbf{r}} = -g\hat{\mathbf{k}} + \frac{p}{m}\hat{\mathbf{k}}_b, \quad (32)$$

$$\dot{\boldsymbol{\omega}} = -\mathbf{J}^{-1}[\boldsymbol{\omega} \times (\mathbf{J}\boldsymbol{\omega})] + \mathbf{J}^{-1}\boldsymbol{\tau}, \quad (33)$$

where  $m, \mathbf{J}$  denote, respectively, mass and mass moment of inertia of the quadcopter.  $g$  is the gravity acceleration and  $p$  is the thrust force generated by the four rotors. Relation

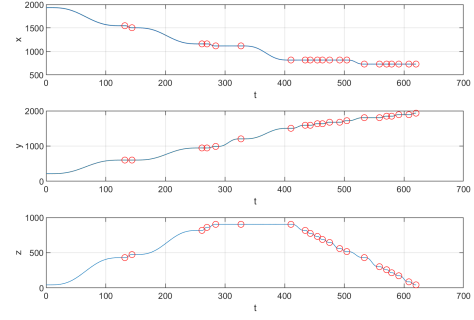


Fig. 8:  $x, y$  and  $z$  components of quadcopters. Red circles show the waypoints.

between the thrust force  $p$  and angular speed of the rotors, denoted by  $\omega_{r_i}$ , can be written as

$$p = \sum_{i=1}^4 f_{r_i} = b \sum_{i=1}^4 \omega_{r_i}^2, \quad (34)$$

where  $b$  is the aerodynamic force constant ( $b$  is a function of the density of air, the shape of the blades, the number of the blades, the chord length of the blades, the pitch angle of the blade airfoil and the drag constant), and  $f_{r_i}$  is the thrust force of  $i^{\text{th}}$  rotor. In (32),  $\boldsymbol{\tau} = [\tau_\phi \ \tau_\theta \ \tau_\psi]^T$  is the control torques generated by four rotors. Relation between the  $\boldsymbol{\tau}$  and angular speed of the rotors can be written in the following form

$$\boldsymbol{\tau} = \begin{bmatrix} \tau_\phi \\ \tau_\theta \\ \tau_\psi \end{bmatrix} = \begin{bmatrix} bl(\omega_{r_4}^2 - \omega_{r_2}^2) \\ bl(\omega_{r_3}^2 - \omega_{r_1}^2) \\ k(\omega_{r_2}^2 + \omega_{r_4}^2 - \omega_{r_1}^2 - \omega_{r_3}^2) \end{bmatrix}, \quad (35)$$

where  $l$  is the distance of each rotor from center of the quadcopter, and  $k$  is a positive constant corresponding to the aerodynamic torques. By concatenating  $p$  and  $\boldsymbol{\tau}$  as input vector to the system, we can write

$$\mathbf{u} = \begin{bmatrix} p \\ \tau_\phi \\ \tau_\theta \\ \tau_\psi \end{bmatrix} = \begin{bmatrix} b & b & b & b \\ 0 & -bl & 0 & bl \\ -bl & 0 & bl & 0 \\ -k & k & -k & k \end{bmatrix} \begin{bmatrix} \omega_{r_1}^2 \\ \omega_{r_2}^2 \\ \omega_{r_3}^2 \\ \omega_{r_4}^2 \end{bmatrix}. \quad (36)$$

By defining state vector  $\mathbf{x} = [\mathbf{r}^T \ \dot{\mathbf{r}}^T \ \phi \ \theta \ \psi \ \boldsymbol{\omega}^T]^T$  and input vector  $\mathbf{u} = [p \ \tau_\phi \ \tau_\theta \ \tau_\psi]^T$ , (32),(33) can be written in the state space non-linear form of

$$\begin{cases} \dot{\mathbf{x}} = \mathbf{f}(\mathbf{x}) + \mathbf{g}(\mathbf{x})\mathbf{u} \\ \mathbf{y} = \mathbf{C}\mathbf{x} \end{cases} \quad (37)$$

where,  $\mathbf{f}(\mathbf{x})$  and  $\mathbf{g}(\mathbf{x})$  are defined as

$$\mathbf{f}(\mathbf{x}) = \begin{bmatrix} \mathbf{v} \\ -g\hat{\mathbf{k}} \\ \mathbf{\Gamma}^{-1}\boldsymbol{\omega} \\ -\mathbf{J}^{-1}[\boldsymbol{\omega} \times (\mathbf{J}\boldsymbol{\omega})] \end{bmatrix}, \quad (38)$$

$$\mathbf{g}(\mathbf{x}) = \begin{bmatrix} \mathbf{0}_{3 \times 1} & \mathbf{0}_{3 \times 3} \\ \frac{\hat{\mathbf{k}}_b}{m} & \mathbf{0}_{3 \times 3} \\ \mathbf{0}_{3 \times 1} & \mathbf{0}_{3 \times 3} \\ \mathbf{0}_{3 \times 1} & \mathbf{J}^{-1} \end{bmatrix} \quad (39)$$

and  $\mathbf{C} = [\mathbf{I}_{3 \times 3}, \mathbf{0}_{3 \times 9}]$ .  $\mathbf{v}$  is the velocity vector of the quadcopter, and  $\mathbf{\Gamma}$  is the matrix which relates Euler angular velocity to the angular velocity of the quadcopter.  $\mathbf{0}_{i \times j}$  is a  $i \times j$  zero matrix. In order to find  $\mathbf{\Gamma}$ , we can represent  $\boldsymbol{\omega}$  in the following form

$$\boldsymbol{\omega} = \dot{\psi} \hat{\mathbf{k}}_1 + \dot{\theta} \hat{\mathbf{j}}_2 + \dot{\phi} \hat{\mathbf{i}}_b, \quad (40)$$

where  $\hat{\mathbf{j}}_2 = \mathbf{R}(\phi, 0, 0) \hat{\mathbf{j}}_b$  and  $\hat{\mathbf{k}}_1 = \mathbf{R}(\phi, \theta, 0) \hat{\mathbf{k}}_b$ . Consequently,

$$\mathbf{\Gamma} = \begin{bmatrix} 1 & 0 & -s_\theta \\ 0 & c_\phi & c_\theta s_\phi \\ 0 & -s_\phi & c_\phi c_\theta \end{bmatrix}. \quad (41)$$

From (40), the angular acceleration  $\dot{\boldsymbol{\omega}}$  can be formulated in the following way:

$$\dot{\boldsymbol{\omega}} = \tilde{\mathbf{B}}_1 [\ddot{\phi} \quad \ddot{\theta} \quad \ddot{\psi}]^T + \tilde{\mathbf{B}}_2 \quad (42)$$

where  $\tilde{\mathbf{B}}_1 = [\hat{\mathbf{i}}_b \quad \hat{\mathbf{j}}_2 \quad \hat{\mathbf{k}}_1]$  and

$$\tilde{\mathbf{B}}_2 = \dot{\theta} \hat{\psi} (\hat{\mathbf{k}}_1 \times \hat{\mathbf{j}}_2) + \dot{\phi} (\hat{\psi} \hat{\mathbf{k}}_1 + \dot{\theta} \hat{\mathbf{j}}_2) \times \hat{\mathbf{i}}_b \quad (43)$$

On the other hand, from (37),

$$\dot{\boldsymbol{\omega}} = \mathbf{J}^{-1} \left( -\boldsymbol{\omega} \times (\mathbf{J} \boldsymbol{\omega}) + [u_2 \quad u_3 \quad u_4]^T \right). \quad (44)$$

From (42) and (44)

$$\begin{bmatrix} u_2 \\ u_3 \\ u_4 \end{bmatrix} = \mathbf{J} \tilde{\mathbf{B}}_1 \begin{bmatrix} \ddot{\phi} \\ \ddot{\theta} \\ \ddot{\psi} \end{bmatrix} + \mathbf{J} \tilde{\mathbf{B}}_2 + \boldsymbol{\omega} \times (\mathbf{J} \boldsymbol{\omega}) \quad (45)$$

### B. Input-Output Feedback Linearization Control

In this subsection, we provide the input control for the non-linear state space system (37) to track the desired trajectory  $\mathbf{r}_d$ . We suppose  $\mathbf{r}_d$  is a smooth function for all  $t \geq t_0$  (i.e.  $\mathbf{r}_d$  has derivatives of all orders with respect to time).

In this work, we use the input-output feedback linearization approach [21] to design the input control for a quadcopter to track the desired trajectory [17]. We use the Lie derivative notation which is defined in the following.

*Definition 1:* Let  $h : \mathbb{R}^n \rightarrow \mathbb{R}$  be a smooth scalar function, and  $\mathbf{f} : \mathbb{R}^n \rightarrow \mathbb{R}^n$  be a smooth vector field on  $\mathbb{R}^n$ . Lie derivative of  $h$  with respect to  $\mathbf{f}$  is a scalar function defined by  $L_{\mathbf{f}} h = \nabla h \mathbf{f}$ .

Concept of input-output linearization is based on differentiating the output until the input appears in the derivative expression. Since  $u_2, u_3$  and  $u_4$  do not appear in the derivative of outputs, we use the technique, called dynamic extension, in which we redefine the input vector  $\mathbf{u}$  as the derivative of some of the original system inputs. In particular, we define  $\tilde{\mathbf{x}} = [\mathbf{x}^T \quad p \quad \dot{p}]^T$  and  $\tilde{\mathbf{u}} = [u_p \quad \tau_\phi \quad \tau_\theta \quad \tau_\psi]^T$ .

Therefore, extended dynamics of the quadcopter can be expressed in the following form [17]:

$$\begin{cases} \dot{\tilde{\mathbf{x}}} = \tilde{\mathbf{f}}(\tilde{\mathbf{x}}) + \tilde{\mathbf{g}}(\tilde{\mathbf{x}}) \tilde{\mathbf{u}} \\ \mathbf{r} = \tilde{\mathbf{C}} \tilde{\mathbf{x}} \end{cases} \quad (46)$$

where,  $\tilde{\mathbf{f}}(\tilde{\mathbf{x}})$  and  $\tilde{\mathbf{g}}(\tilde{\mathbf{x}})$  are defined as

$$\tilde{\mathbf{f}}(\tilde{\mathbf{x}}) = \begin{bmatrix} \mathbf{f}(\mathbf{x}) \\ \dot{p} \\ 0 \end{bmatrix} + \begin{bmatrix} \mathbf{0}_{3 \times 1} \\ \frac{p}{m} \hat{\mathbf{k}}_b \\ \mathbf{0}_{8 \times 1} \end{bmatrix}, \quad (47)$$

$$\tilde{\mathbf{g}}(\tilde{\mathbf{x}}) = \begin{bmatrix} \mathbf{0}_{9 \times 1} & \mathbf{0}_{9 \times 3} \\ \mathbf{0}_{3 \times 1} & \mathbf{J}^{-1} \\ 0 & \mathbf{0}_{1 \times 3} \\ 1 & \mathbf{0}_{1 \times 3} \end{bmatrix}. \quad (48)$$

Let  $\tilde{\mathbf{g}}_i(\tilde{\mathbf{x}})$  denote the  $i^{\text{th}}$  column of matrix  $\tilde{\mathbf{g}}(\tilde{\mathbf{x}})$  and  $\tilde{\mathbf{u}} = [\tilde{u}_1 \dots \tilde{u}_4]^T$  where  $\tilde{u}_1, \dots, \tilde{u}_4$  corresponds to  $u_p, \tau_\phi, \tau_\theta, \tau_\psi$ , respectively. We consider the position of the quadcopter as the output of the system (i.e.  $x, y, z$ ). Inputs appear in the fourth order derivative of the outputs. particularly, for  $q \in \{x, y, z\}$

$$\ddot{\ddot{q}} = L_{\tilde{\mathbf{f}}}^4 q + \sum_{i=1}^4 L_{\tilde{\mathbf{g}}_i} L_{\tilde{\mathbf{f}}}^3 q \tilde{u}_i \quad (49)$$

where  $L_{\tilde{\mathbf{g}}_i} L_{\tilde{\mathbf{f}}}^3 q \neq 0$  for  $i = 1, \dots, 4$ . By choosing the state transformation  $\mathcal{T}(\tilde{\mathbf{x}}) = [\mathbf{z} \quad \boldsymbol{\zeta}]^T$ , (46) can be converted to the following internal and external dynamics:

$$\dot{\boldsymbol{\zeta}} = \begin{bmatrix} 0 & 0 \\ 0 & 1 \end{bmatrix} \boldsymbol{\zeta} + \begin{bmatrix} 0 \\ 1 \end{bmatrix} u_\psi \quad (50)$$

$$\dot{\mathbf{z}} = \mathbf{A} \mathbf{z} + \mathbf{B} \mathbf{s} \quad (51)$$

where  $\mathbf{z} = [\mathbf{r}^T \quad \dot{\mathbf{r}}^T \quad \ddot{\mathbf{r}}^T \quad \ddot{\mathbf{r}}^T]^T$ , and  $\boldsymbol{\zeta} = [\psi \quad \dot{\psi}]^T$

$$\mathbf{A} = \begin{bmatrix} \mathbf{0}_{9 \times 3} & \mathbf{I}_9 \\ \mathbf{0}_{3 \times 3} & \mathbf{0}_{3 \times 9} \end{bmatrix}, \mathbf{B} = \begin{bmatrix} \mathbf{0}_{9 \times 3} \\ \mathbf{I}_3 \end{bmatrix} \quad (52)$$

where  $\mathbf{I}_j$  is a  $j \times j$  identity matrix.

Next, we can figure out the Control inputs  $\mathbf{s}$  and  $u_\psi$ , such that the linear systems (50) and (51) track the desired trajectory  $\mathbf{r}_d$ . By choosing

$$u_\psi = -K_1 \dot{\psi} - K_2 \psi \quad (53)$$

where  $K_1 > 0, K_2 > 0$ . Thus, the internal dynamics (50) asymptotically converges to  $\mathbf{0}$ . Moreover, we choose

$$\mathbf{s} = K_3 (\ddot{\mathbf{r}}_d - \ddot{\mathbf{r}}) + K_4 (\ddot{\mathbf{r}}_d - \ddot{\mathbf{r}}) + K_5 (\dot{\mathbf{r}}_d - \dot{\mathbf{r}}) + K_6 (\mathbf{r}_d - \mathbf{r}) \quad (54)$$

where  $K_3, \dots, K_6$  can be chosen such that the roots of the characteristic equation

$$\lambda^4 + \lambda^3 K_3 + \lambda^2 K_4 + \lambda K_5 + K_6 = 0, \quad (55)$$

are located in the open left half complex plane. Hence,  $\mathbf{r}$  converges to  $\mathbf{r}_d$ .

In order to find the relation between  $s$  and  $\tilde{u}$ , we need to find  $\ddot{r}$  by differentiating twice with respect to time from  $\dot{r}$ . From (37), we have

$$\ddot{r} = \frac{p}{m} \hat{k}_b - g \hat{k} \quad (56)$$

By differentiating the above expression,

$$\ddot{r} = \frac{\dot{p}}{m} \hat{k}_b + \frac{p}{m} \omega \times \hat{k}_b \quad (57)$$

$$\ddot{r} = \frac{1}{m} (O_1 \Theta + O_2), \quad (58)$$

where  $\Theta = [\ddot{p} \quad \ddot{\phi} \quad \ddot{\theta} \quad \ddot{\psi}]^T$  and

$$O_1 = [\hat{k}_b \quad -p\hat{j}_b \quad p(\hat{j}_2 \times \hat{k}_b) \quad p(\hat{k}_1 \times \hat{k}_b)] \quad (59)$$

$$O_2 = p\tilde{B}_2 \times \hat{k}_b + \omega \times (\omega \times p\hat{k}_b) + 2\dot{p}\omega \times \hat{k}_b \quad (60)$$

where  $\tilde{B}_2$  is defined in (43). From (45),  $\Theta$  can be written in the form of

$$\Theta = O_3 \tilde{u} + O_4, \quad (61)$$

where

$$O_3 = \begin{bmatrix} 1 & \mathbf{0}_{1 \times 3} \\ \mathbf{0}_{1 \times 3} & J^{-1} \tilde{B}_1^{-1} \end{bmatrix}, \quad (62)$$

$$O_4 = \begin{bmatrix} 0 \\ -\tilde{B}_1^{-1} \tilde{B}_2 - J^{-1} \omega \times (J\omega) \end{bmatrix}. \quad (63)$$

Substituting (61) in (58)

$$s = \frac{1}{m} (O_1 O_3 \tilde{u} + O_1 O_4 + O_2) \quad (64)$$

## REFERENCES

- [1] K. Peng, G. Cai, B. M. Chen, M. Dong, K. Y. Lum, and T. H. Lee, "Design and implementation of an autonomous flight control law for a uav helicopter," *Automatica*, vol. 45, no. 10, pp. 2333–2338, 2009.
- [2] B. Argrow, D. Lawrence, and E. Rasmussen, "Uav systems for sensor dispersal, telemetry, and visualization in hazardous environments," in *43rd AIAA Aerospace Sciences Meeting and Exhibit*, 2005, p. 1237.
- [3] D. C. Tsouros, S. Bibi, and P. G. Sarigiannidis, "A review on uav-based applications for precision agriculture," *Information*, vol. 10, no. 11, p. 349, 2019.
- [4] A. Puri, "A survey of unmanned aerial vehicles (uav) for traffic surveillance," *Department of computer science and engineering, University of South Florida*, pp. 1–29, 2005.
- [5] H. Surmann, R. Worst, T. Buschmann, A. Leinweber, A. Schmitz, G. Senkowski, and N. Goddemeier, "Integration of uavs in urban search and rescue missions," in *2019 IEEE International Symposium on Safety, Security, and Rescue Robotics (SSRR)*. IEEE, 2019, pp. 203–209.
- [6] J. Witzczuk, S. Pagacz, A. Zmarz, and M. Cypel, "Exploring the feasibility of unmanned aerial vehicles and thermal imaging for ungulate surveys in forests-preliminary results," *International Journal of Remote Sensing*, vol. 39, no. 15–16, pp. 5504–5521, 2018.
- [7] B. Arbanas, A. Ivanovic, M. Car, T. Haus, M. Orsag, T. Petrovic, and S. Bogdan, "Aerial-ground robotic system for autonomous delivery tasks," in *2016 IEEE international conference on robotics and automation (ICRA)*. IEEE, 2016, pp. 5463–5468.
- [8] T. Bailey and H. Durrant-Whyte, "Simultaneous localization and mapping (slam): Part ii," *IEEE robotics & automation magazine*, vol. 13, no. 3, pp. 108–117, 2006.
- [9] M. Betke and L. Gurvits, "Mobile robot localization using landmarks," *IEEE transactions on robotics and automation*, vol. 13, no. 2, pp. 251–263, 1997.
- [10] H. Rastgoftar, S. Nersesov, and H. Ashrafiuon, "Continuum deformation coordination of multi-agent systems using cooperative localization," *arXiv preprint arXiv:2104.09998*, 2021.
- [11] R. Sharma and C. Taylor, "Vision based distributed cooperative navigation for mavs in gps denied areas," in *AIAA Infotech@ Aerospace Conference and AIAA Unmanned... Unlimited Conference*, 2009, p. 1932.
- [12] J. S. Jennings, G. Whelan, and W. F. Evans, "Cooperative search and rescue with a team of mobile robots," in *1997 8th International Conference on Advanced Robotics. Proceedings. ICAR'97*. IEEE, 1997, pp. 193–200.
- [13] R. Sharma, R. W. Beard, C. N. Taylor, and D. Pack, "Bearing-only cooperative geo-localization using unmanned aerial vehicles," in *2012 American Control Conference (ACC)*. IEEE, 2012, pp. 3883–3888.
- [14] S. S. Kia, S. Rounds, and S. Martinez, "Cooperative localization for mobile agents: A recursive decentralized algorithm based on kalman-filter decoupling," *IEEE Control Systems Magazine*, vol. 36, no. 2, pp. 86–101, 2016.
- [15] A. Howard, M. J. Matark, and G. S. Sukhatme, "Localization for mobile robot teams using maximum likelihood estimation," in *IEEE/RSJ international conference on intelligent robots and systems*, vol. 1. IEEE, 2002, pp. 434–439.
- [16] E. D. Nerurkar, S. I. Roumeliotis, and A. Martinelli, "Distributed maximum a posteriori estimation for multi-robot cooperative localization," in *2009 IEEE International Conference on Robotics and Automation*. IEEE, 2009, pp. 1402–1409.
- [17] H. Rastgoftar and I. V. Kolmanovsky, "Safe affine transformation-based guidance of a large-scale multi-quadcopter system (mqcs)," *IEEE Transactions on Control of Network Systems*, 2021.
- [18] H. Rastgoftar, E. M. Atkins, and D. Panagou, "Safe multiquadcopter system continuum deformation over moving frames," *IEEE Transactions on Control of Network Systems*, vol. 6, no. 2, pp. 737–749, 2018.
- [19] D. Simon, *Optimal state estimation: Kalman, H infinity, and nonlinear approaches*. John Wiley & Sons, 2006.
- [20] P. E. Hart, N. J. Nilsson, and B. Raphael, "A formal basis for the heuristic determination of minimum cost paths," *IEEE transactions on Systems Science and Cybernetics*, vol. 4, no. 2, pp. 100–107, 1968.
- [21] J.-J. E. Slotine, W. Li *et al.*, *Applied nonlinear control*. Prentice hall Englewood Cliffs, NJ, 1991, vol. 199, no. 1.